ACS OMEGA

Open Access

http://pubs.acs.org/journal/acsodf

Article

Study for Hydrogen Migration Characteristics in the Elbow of a Hydrogen-Doped Natural Gas Pipeline under Normal Transport and Shutdown Conditions

Jiuqing Ban, Li Zhou, Yun Jiang, Yan Wu, Wei Yang, Duo Chen, and Gang Liu*

Cite This: ACS Omega 2024, 9, 47621−47636

Read Online

ACCESS | Metrics & More | Article Recommendations

ABSTRACT: During the transportation of hydrogen-doped natural gas (HCNG), there is a risk of uneven distribution of hydrogen at the elbow, causing hydrogen damage to the pipeline. Therefore, based on the basic principles of computational fluid dynamics, this paper uses a hybrid model to describe the flow process of HCNG in an elbow. The results show that under normal transportation, the hydrogen volume fraction varies within 0.2% with the influence of pressure, flow velocity, temperature, hydrogen volume fraction, and undulating angle, and the uneven distribution of hydrogen in the elbow can be ignored. However, in the shutdown state, the hydrogen slip rate gradually slows down, the hydrogen volume fraction is distributed in a horizontal concentration gradient along the vertical direction, and it gradually accumulates at the height of the undulating tube. The difference in hydrogen volume fraction reaches 50%, and the stratification phenomenon is obvious.

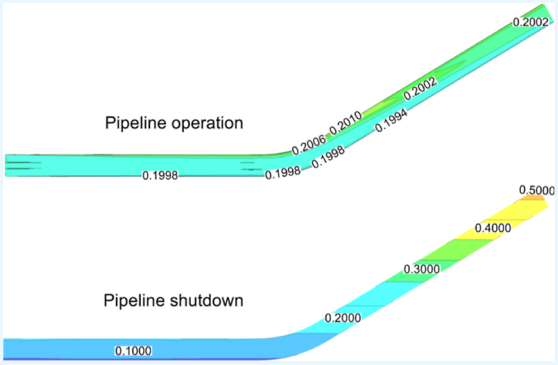

1. INTRODUCTION

With global warming, the energy crisis, the acceleration of energy processes, and the development of environment protection concepts, China's energy structure has gradually changed from fossil energy such as kerosene and gas to renewable energy such as hydrogen energy.[1−3] Hydrogen energy has the advantages of being clean, zero-carbon, and having high energy storage density. It is a high-quality renewable and clean energy carrier.[4−6] It occupies an important position in the current energy structure and is regarded as the greatest potential energy in the 21st century.[7] It plays an important role in achieving "carbon peak, carbon neutrality".[8−11] In the process of developing hydrogen energy, the large-scale and long-distance transportation of hydrogen is a key problem that urgently needs to be solved urgently. At present, the main transportation modes of hydrogen energy include liquid hydrogen tank truck transportation,[12−14] pure hydrogen pipeline transportation,[15−17] and natural gas pipeline transportation.[18−20] Among them, the cost of using a liquid hydrogen tank truck to transport hydrogen energy is high. The construction of a pure hydrogen pipeline requires special basic equipment, such as a hydrogen pipeline and compressor, which is very expensive and takes a lot of time.[21,22] Incorporating hydrogen into existing natural gas pipeline transportation is the most cost-effective method, and it is also the main means of transporting hydrogen in the future.[23−26]

Most of the existing natural gas pipelines or pipelines under construction are high-grade pipelines. High-grade steel pipeline has high strength, low temperature crack arrest toughness, and good weldability. These characteristics can reduce the maintenance cost of long-distance pipelines and achieve the ability to transport gas under higher pressure.[27] High-grade pipelines are more susceptible to hydrogen embrittlement than low-grade pipelines.[28] Due to the different physical and chemical properties of hydrogen and natural gas, the complex flow characteristics in the pipeline may lead to the phenomenon of stratified flow under the action of gravity and pressure mutation. The hydrogen forms a high concentration accumulation area in the local part of the pipeline, resulting in nonuniform concentration field distribution. Hydrogen can change the mechanical properties of steel, such as strength, toughness, plasticity, etc., causing hydrogen damage and pipeline failure.[29,30]

The flow characteristics of HCNG in different types of pipelines are different, and the areas of high concentration accumulation of hydrogen are also different. When HCNG

Received: July 30, 2024
Revised: August 24, 2024
Accepted: October 16, 2024
Published: November 19, 2024

https://doi.org/10.1021/acsomega.4c06890
ACS Omega 2024, 9, 47621−47636

flows in a T-shaped pipeline, An et al.[31] and Wang et al.[32] found that hydrogen accumulates above the pipeline. When the flow velocity of the variable diameter mixing T-shaped pipeline is small, it is easy to cause hydrogen accumulation. The closer the mixing center, the more obvious the stratification phenomenon. When the HCNG flows in the undulating pipe, Liu et al. and Li et al.[33] found that the gas has obvious stratification in front of the undulating pipe. In the case of low speed, low temperature, and high pressure, it is beneficial to increase the hydrogen volume fraction after stratification. When HCNG flows in a horizontal pipe, Liu et al.[34] found that hydrogen is easy to accumulate above the pipeline. The lower the temperature, the smaller the flow velocity, the greater the pressure, and the more obvious the stratification phenomenon. When hydrogen flows in spiral pipes with different turns and different diameter positions, Ji et al.[35] found that there is obvious stratification at the outlet of the spiral pipeline, and the mixing becomes more uniform with the increase of distance. These studies confirmed that there is a certain stratification phenomenon in the flow of HCNG in the pipeline. The gas flow characteristics at the elbow are complex and have huge risks. The distribution of the hydrogen concentration is not systematically explained clearly, which is worthy of further study.

When the pipeline encounters an accident and needs to be shut down for maintenance, the flow state of the HCNG in the pipeline is more stable, making it easier for hydrogen to accumulate. Marangon et al.[36] explored the static stratification of 10 and 30% HCNG with or without natural ventilation in a 25m3 hexahedral container. The results showed that nonuniform mixture concentration and stratification were observed in the experiment. Ren,[37,38] explored the concentration distribution of methane and air in small-volume containers through cylindrical containers combined with software Fluent. It was found that there was a stratification phenomenon, and the stratification of small containers was more obvious than that of large containers. Chen et al.[39] studied the stratification of 10% HCNG in the undulating pipe and horizontal pipe under the condition of shutdown for 50 min. The results showed that the difference of hydrogen volume concentration between the high and low points of the undulating pipe was about 2%, and the hydrogen concentration at the top of the horizontal pipe was about 1.8 times that at the bottom. Liu et al.[34] found that HCNG in the gas storage cylinder and horizontal pipe in the static process showed stratification through simulation research. With the increase of pressure and hydrogen volume fraction and the decrease of temperature and pipe diameter, the stratification phenomenon is more obvious. Zhu et al.[40] studied the effect of undulating height on the standing of HCNG in undulating pipe. The results show that as the undulating height increases, the longer the hydrogen reaches a stable stratification and the greater the hydrogen concentration, the more obvious the stratification.

At present, domestic and foreign scholars have made a preliminary exploration on the distribution of hydrogen concentration in HCNG under the operation or shutdown of a T-shaped pipeline and undulating pipe. They revealed the influence of pressure, flow velocity, hydrogen volume fraction, and other influencing factors on the distribution of hydrogen and put forward corresponding preventive measures for the high-concentration hydrogen accumulation area. However, there are few studies on the distribution of the hydrogen concentration in the elbow, and hydrogen is more likely to accumulate at the elbow during the transportation process. It is easier to stratify in the static state than in the flow state, and the harm to the pipeline is also greater. Therefore, it is urgent to explore the change law of the hydrogen concentration distribution field in the elbow. Based on the basic principle of computational fluid dynamics, this paper focuses on the variation of hydrogen concentration distribution in elbows under different pressures, flow velocities, hydrogen volume fractions, temperatures, and other influencing factors. The variation of the hydrogen concentration distribution of HCNG in elbows from operation to shutdown was also studied. The calculation results can provide theoretical support for the maintenance of the HCNG from operation to shutdown.

2. NUMERICAL METHODS

2.1. Mathematical Model. The continuity equation of natural gas and hydrogen in the mixing process is

$$\frac{\partial \rho}{\partial t} + \frac{\partial(\rho\omega_x)}{\partial x} + \frac{\partial(\rho\omega_y)}{\partial y} + \frac{\partial(\rho\omega_z)}{\partial z} = 0 \tag{1}$$

where ρ is the density of the fluid, kg/m^3; t is the time, s; and ω_x, ω_y, and ω_z are the component of the velocity in x, y, z directions, m/s.

The momentum equation of natural gas and hydrogen in the mixing process is

$$\frac{\partial(pu_x)}{\partial t} + \nabla(pu_x\vec{u}) = -\frac{\partial p}{\partial x} + \frac{\partial \tau_{xx}}{\partial x} + \frac{\partial \tau_{yx}}{\partial y} + \frac{\partial \tau_{zx}}{\partial z} + pf_x \tag{2}$$

$$\frac{\partial(pu_y)}{\partial t} + \nabla(pu_y\vec{u}) = -\frac{\partial p}{\partial y} + \frac{\partial \tau_{xy}}{\partial x} + \frac{\partial \tau_{yy}}{\partial y} + \frac{\partial \tau_{zy}}{\partial z} + pf_y \tag{3}$$

$$\frac{\partial(pu_z)}{\partial t} + \nabla(pu_z\vec{u}) = -\frac{\partial p}{\partial z} + \frac{\partial \tau_{xz}}{\partial x} + \frac{\partial \tau_{yz}}{\partial y} + \frac{\partial \tau_{zz}}{\partial z} + pf_z \tag{4}$$

where p is the absolute pressure, Pa; τ_{xx}, τ_{xy}, and τ_{xz} are the component of viscous stress, Pa·s; and f_x, f_y, and f_z are the unit mass force, m·s^{-2}.

The energy equation of natural gas and hydrogen in the mixing process is

$$\frac{\partial(pT)}{\partial t} + \frac{\partial(pu_xT)}{\partial x} + \frac{\partial(pu_yT)}{\partial y} + \frac{\partial(pu_zT)}{\partial z} = \frac{\partial}{\partial x}\left(\frac{k}{c_p}\frac{\partial T}{\partial x}\right) + \frac{\partial}{\partial y}\left(\frac{k}{c_p}\frac{\partial T}{\partial y}\right) + \frac{\partial}{\partial z}\left(\frac{k}{c_p}\frac{\partial T}{\partial z}\right) + S_T \tag{5}$$

where c_p is the specific heat capacity, J·mol^{-1}·K^{-1}; T is the gas temperature, K; k is the heat transfer coefficient, W·m^{-2}·K^{-1}; and S_T is the viscous dissipation term.

The flow of HCNG in the elbow belongs to turbulent flow. The standard k-ε two-equation turbulence model is used to close the equations. The turbulent kinetic energy equation k is expressed as

https://doi.org/10.1021/acsomega.4c06890
ACS Omega 2024, 9, 47621−47636

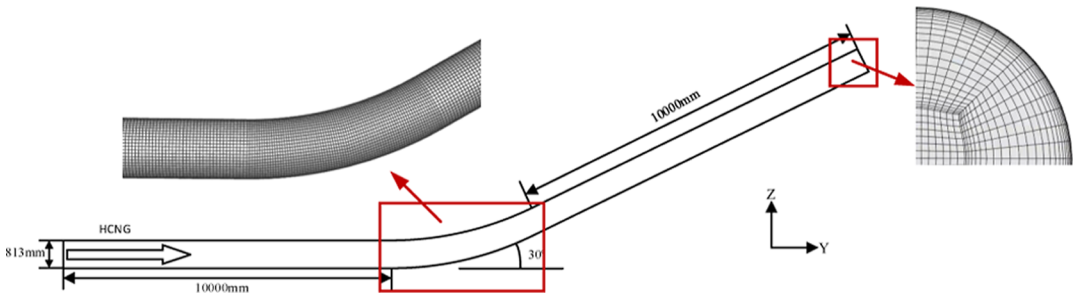

Figure 1. Local division diagram of elbow grid.

Table 1. Grid Independence Verification Monitoring Point Coordinates

monitoring points/(m)	1	2	3	4	5	6	7	8	9
X	0	0	0	0	0	0	0	0	0
Y	1	2	3	4	5	6	7	8	9
Z	0.4	0.4	0.4	0.4	0.4	0.4	0.4	0.4	0.4

$$\frac{\partial(\rho k)}{\partial t} + \frac{\partial(\rho k u_i)}{\partial u_i} = \frac{\partial}{\partial x_j}\left[\left(\mu + \frac{\mu_i}{\sigma_k}\right)\frac{\partial k}{\partial x_j}\right] + G_k + G_b - \rho\varepsilon - Y_s \quad (6)$$

The turbulent kinetic energy dissipation equation ε is expressed as

$$\frac{\partial}{\partial t}(\rho_m \varepsilon) + \nabla\cdot(\rho_m \varepsilon v_m) = V\cdot\left[\left(\mu_m + \frac{\mu_t}{\sigma_\varepsilon}\right)\frac{\partial \varepsilon}{\partial x_j}\right] + C_{1\varepsilon}\frac{\varepsilon}{k}(G_k + C_{3\varepsilon}G_b) - C_{2\varepsilon}\rho_m\frac{\varepsilon^2}{k} \quad (7)$$

of which

$$\mu_t = \rho C_\mu \frac{k^2}{\varepsilon}$$

where k is the turbulent flow energy, J; ε is the turbulent energy dissipation rate, %; μ_t is the turbulent viscosity, m^2/s; G_k is the turbulent kinetic energy generated by the velocity gradient; G_b is the turbulent kinetic energy generated by buoyancy; and Y_s is the source term caused by wave expansion in compressible fluid, where σ_k, σ_ε, $C_{1\varepsilon}$, $C_{2\varepsilon}$, and C_μ are constants.

2.2. Geometry and Meshing. Referring to the actual pipeline parameters of a research institute, the undulating elbow model is established by using computational fluid dynamics software. The diameter of the model is 813 mm, the horizontal pipe length is 10 m, the undulating pipe length is 10 m, and the angle with the horizontal plane is 30°.

The 3D hexahedral structured meshing of the elbow model uses ICEM. The denser the mesh, the closer the calculation result is to the real solution, but it will also increase the calculation scale. In order to improve the accuracy of the calculation, the wall and the elbow are encrypted, and the local schematic diagram of the mesh is shown in Figure 1. A monitoring point is set inside the elbow to monitor the change of hydrogen volume fraction with time, and the coordinates of the monitoring point are shown in Table 1. The data collected by the monitoring point are the area weighted average of the volume fraction (the monitoring points in the following text are the same as above). In order to improve the computational efficiency, the grid independence is verified by setting different grid sizes, and the number of grids is 470,400, 810,040, 1,275,000, 1,755,182, and 2,633,040. The change curve of hydrogen volume fraction with *Y* direction coordinates at the monitoring point is shown in Figure 2. From Figure 2, it can be seen that the hydrogen volume fraction change curves of the 1,755,182 grid and 2,633,040 grid are basically coincident. Considering the calculation accuracy and calculation time, 1,755,182 grid is selected for simulation.

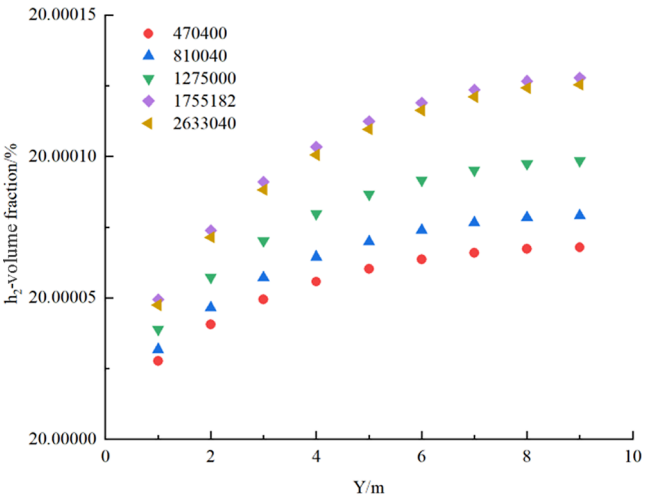

Figure 2. Grid independence verification.

2.3. Model Validation. To ensure the accuracy of the simulation results, the experiment of Ren,[37,38] was compared using the same multiphase flow mixture model, SIMPLE algorithm, boundary conditions, and calculation settings as the experiment. The methane concentration at 1/5 and 4/5 of the tank height was observed after standing for 5 min. The simulation value and the experiment are listed in Figure 3.

From Figure 3, the simulation results are in good agreement with the experimental results, indicating that the numerical model in this paper is reliable.

https://doi.org/10.1021/acsomega.4c06890
ACS Omega 2024, 9, 47621−47636

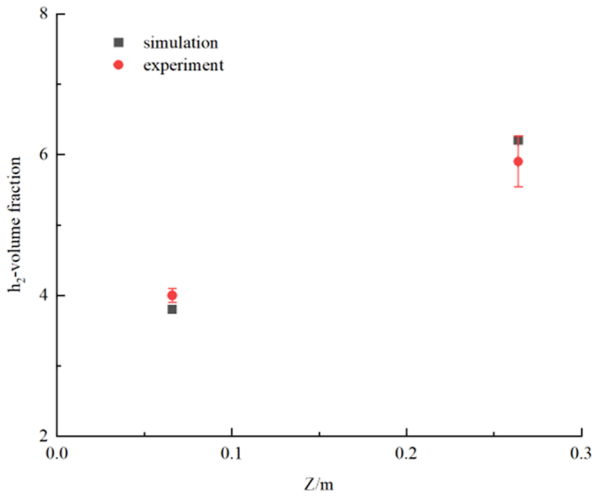

Figure 3. Model validation.

3. STUDY ON THE DISTRIBUTION OF HYDROGEN CONCENTRATION UNDER THE OPERATION OF ELBOWS

3.1. Analysis of Elbow Flow Characteristics. In this paper, ANSYS fluent is used for simulation calculation. In the process of simulation, heat transfer with the outside world is not considered. The pipe wall is the adiabatic wall boundary. The gravitational acceleration of the Z axis is set to be −9.8 m·s^{-1}. The boundary conditions of the model are shown in Table 2, and methane is used instead of natural gas in the simulation process. The long-distance HCNG pipeline has a high pressure and fast flow velocity. According to the adaptability of the HCNG pipeline and related standards,[41,42] referring to the actual working conditions of a research institute, the operating parameters of the elbow are designed, as shown in Table 3. The simulation results are imported into Tecplot360 software for postprocessing analysis to obtain the velocity contours of the cross-section of the elbow, as shown in Figure 4.

Table 2. Model Boundary Condition

the name of the boundary	model location	boundary conditions
inlet	pipe inlet	velocity-inlet
outlet	pipe outlet	pressure-outlet
wall-G	pipe wall	wall

Table 3. Elbow Operation Parameters

gas flow velocity/(m/s)	pipeline pressure/(MPa)	ambient temperature/(K)	hydrogen volume fraction/(%)
7	4.5	293.15	20

From Figure 4, it can be seen that at the horizontal pipe the center velocity of the pipe is basically about 7.0 m/s. At the elbow and undulating pipe, due to the inertia, the hydrogen flow velocity is faster at the upper part of the elbow and the lower part of the undulating pipe, and the flow velocity at the upper part of the undulating pipe is about 6.0 m/s. Due to the roughness of the pipe wall, hydrogen is viscous, and there is resistance at the pipe wall. The closer to the wall, the lower the velocity.

The hydrogen volume fraction distribution contour and pressure contour of the cross-section of the pipeline are shown in Figure 5. From Figure 5, as HCNG enters the elbow, methane gradually accumulates downward during the flow of the pipeline, and the hydrogen gradually accumulates upward in the pipeline, forming a stratification phenomenon. This is because the density of methane is greater than that of hydrogen and the mass is heavier than air. The closer to the center of the pipeline, the more uniform the hydrogen distribution. At the elbow, due to the action of inertial force, the stratification phenomenon is more obvious. At the undulating pipe section, due to the influence of gravity, the higher the height, the easier the hydrogen is to accumulate.

As can be seen from the pressure contour, due to the stratification of methane and hydrogen in the elbow, the pressure distribution in the elbow is stratified. At the horizontal pipe section, the pressure at the top of the pipe is less than that at the bottom of the pipe, and the pressure stratification at the elbow is greater than that at the horizontal pipe section. At the undulating pipe section, the pressure gradually decreases with an increase of height.

3.2. Analysis of Influencing Factors. Based on the above working conditions, the changes of hydrogen flow in the elbow under different pressures, flow velocities, temperatures, hydrogen volume fractions, and undulating angles were investigated. In order to further study the flow phenomenon of HCNG in the elbow, the specific working conditions are shown in Table 4. Monitoring points are set inside the elbow to monitor the change in hydrogen volume fraction with time. The coordinates of monitoring points are shown in Table 5.

3.2.1. Effect of Different Pressures on the Flow of Hydrogen in the Elbow. Select group 1 to explore the influence of different pressures on the flow of hydrogen in the elbow. Keeping other conditions unchanged, increase the pressure from 3.5 to 5.5 MPa. The maximum hydrogen volume fraction under different pressures and the gradient changes of hydrogen volume fraction in gravity direction at the outlet are shown in Table 6. Figure 6 shows the variation curve of the hydrogen volume fraction with Y-axis coordinates at the monitoring point and the gradient curve of the hydrogen volume fraction at the outlet. Figure 7 shows the contours of the hydrogen volume fraction at Y = 12 m and elbow.

From Table 6 and Figures 6 and 7, when the pressure increases from 3.5 to 5.5 MPa, the maximum hydrogen volume fraction increases from 20.1233 to 20.2040%. At the horizontal pipe, because the density of methane is larger than that of hydrogen, under the influence of gravity, hydrogen gradually accumulates on the upper surface of the pipe along the direction of pipe length, and the hydrogen volume fraction is higher at the end of the pipe. The stratification phenomenon is more obvious with the increase of pressure. The hydrogen volume fraction gradient in the gravity direction at the outlet increases from 0.1136 to 0.1827. At the elbow, the stratification phenomenon is more obvious with the increase of pressure. This is because the increase in pressure will increase the density of the gas, the distance between the gas molecules will shorten, resulting in an increase in the number of gas molecules in the unit volume, making the gas stratification more obvious. Therefore, in order to avoid stratification, HCNG is suitable for operation at low pressure.

3.2.2. Effect of Different Flow Velocities on the Flow of Hydrogen in the Elbow. Select group 2 to explore the influence of different flow velocities on the flow of hydrogen in the elbow. Keeping other conditions unchanged, increase the flow velocity from 5 to 9 m/s. The maximum hydrogen volume

https://doi.org/10.1021/acsomega.4c06890
ACS Omega 2024, 9, 47621−47636

Figure 4. Velocity contours.

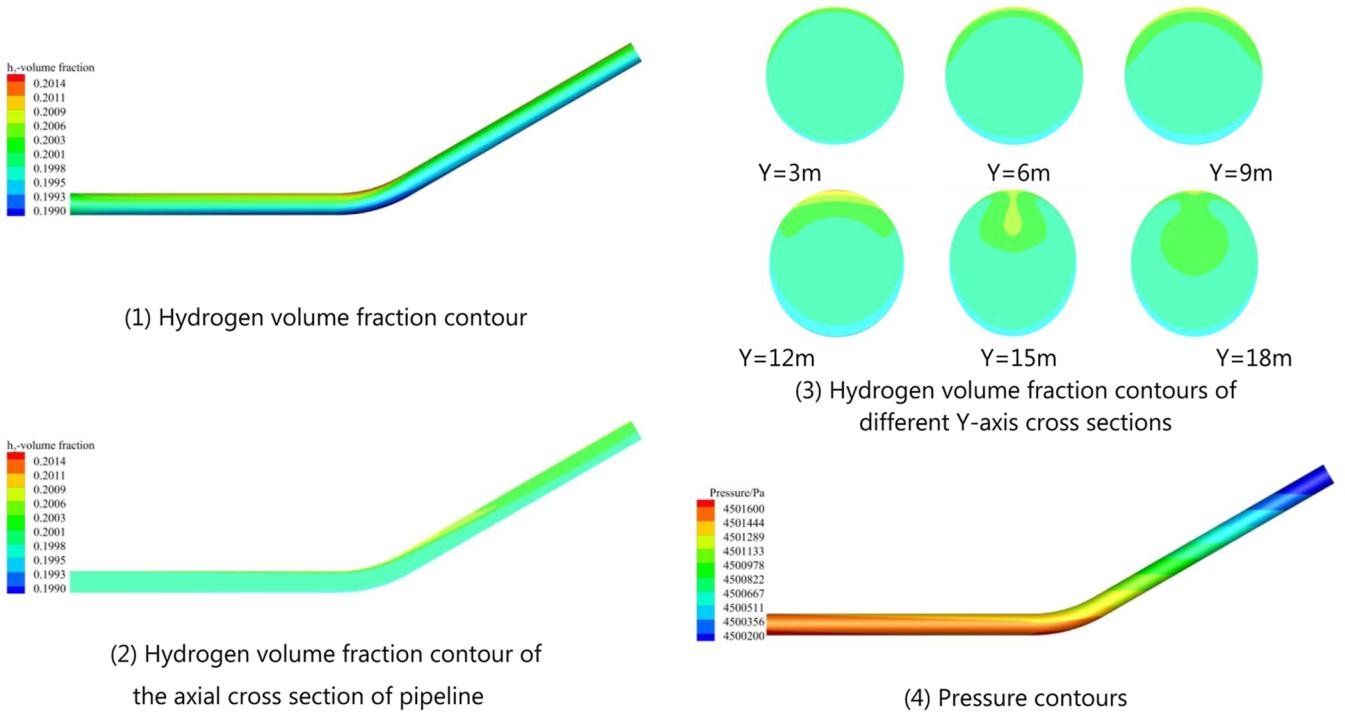

Figure 5. Hydrogen volume fraction and pressure contours.

Table 4. Work Condition

group	pressure/(MPa)	flow velocity/(m/s)	temperature/(°C)	hydrogen volume fraction/(%)	undulating angle/(deg)
1	3.5, 4.0, 4.5, 5.0, 5.5	7.0	20	20	30
2	4.5	6.0, 7.0, 8.0, 9.0, 10.0	20	20	30
3	4.5	7.0	0, 10, 20, 30, 40	20	30
4	4.5	7.0	20	10, 15, 20, 25, 30	30
5	4.5	7.0	20	20	30, 45, 60

Table 5. Monitoring Point Coordinates

monitoring point/(m)	1	2	3	4	5	6	7	8	9	10
X	0	0	0	0	0	0	0	0	0	0
Y	1	2	3	4	5	6	7	8	9	10
Z	0.405	0.405	0.405	0.405	0.405	0.405	0.405	0.405	0.405	0.405

Table 6. Change of the Maximum Hydrogen Volume Fraction under Different Pressures

influencing factor	pressure/(MPa)	maximum hydrogen volume fraction/(%)	hydrogen volume in gravity direction/(10^{-2} m^{-1})
pressure	3.5	20.1233	0.1136
	4.0	20.1427	0.1310
	4.5	20.1628	0.1484
	5.0	20.1835	0.1655
	5.5	20.2040	0.1827

https://doi.org/10.1021/acsomega.4c06890
ACS Omega 2024, 9, 47621−47636

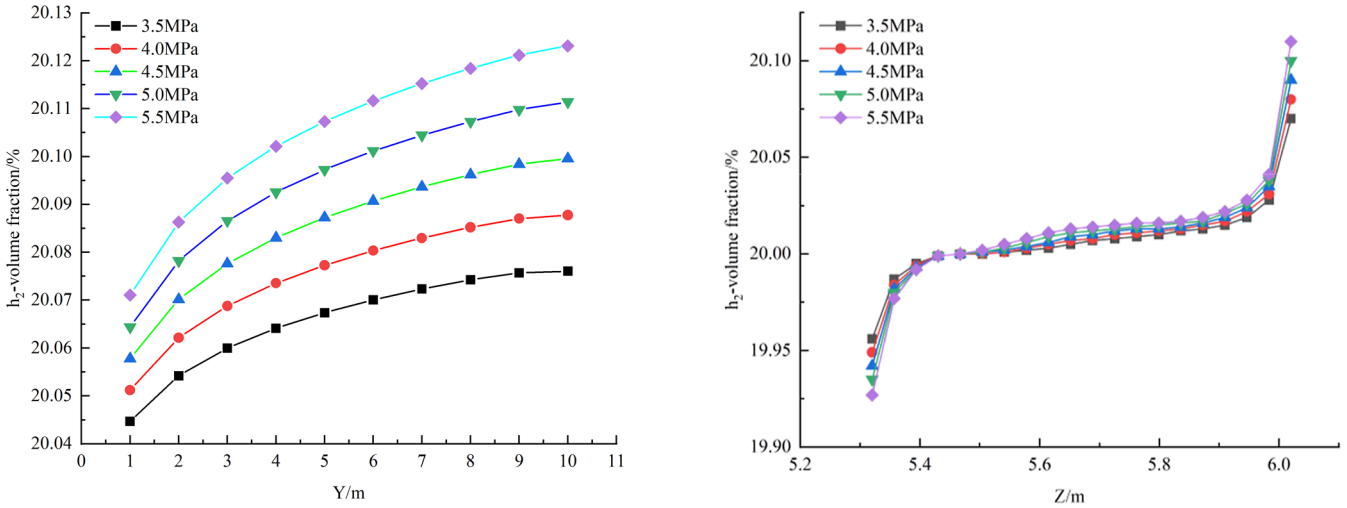

Figure 6. Variation curve of hydrogen volume fraction with *Y*-axis coordinates and the gradient diagram of hydrogen volume fraction under different pressures.

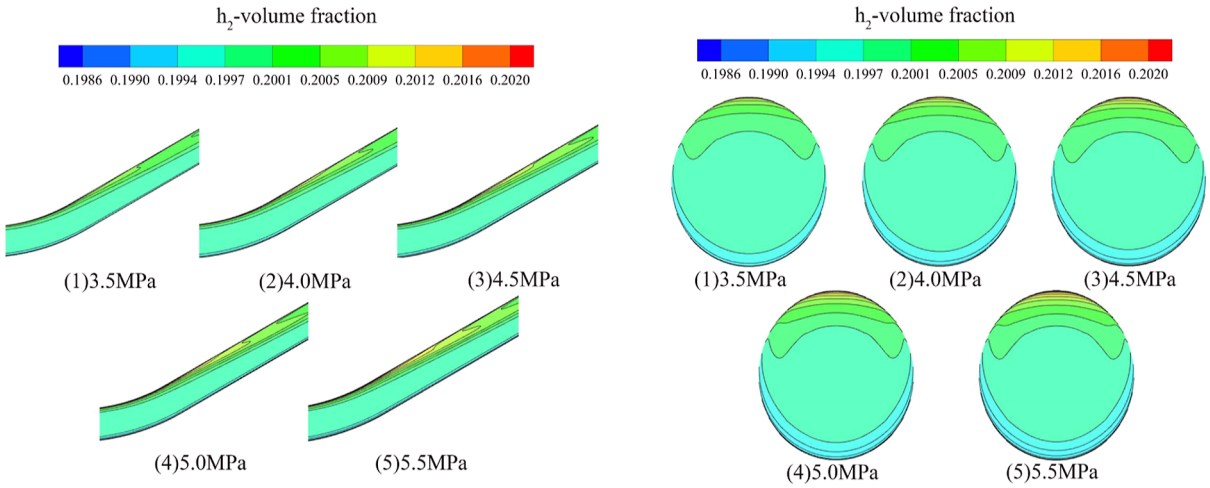

Figure 7. Distribution contours of hydrogen volume fraction at elbow under different pressures.

Table 7. Change of the Maximum Hydrogen Volume Fraction under Different Flow Velocities

influencing factor	flow velocity/(m/s)	maximum hydrogen volume fraction/(%)	hydrogen volume in gravity direction/(10^{-2} m^{-1})
flow velocity	6	20.1757	0.1722
	7	20.1628	0.1484
	8	20.1559	0.1303
	9	20.1525	0.1160
	10	20.1520	0.1048

fraction under different flow velocities and the gradient changes of the hydrogen volume fraction in gravity direction at the outlet are shown in Table 7. Figure 8 shows the variation curve of hydrogen volume fraction with *Y*-axis coordinates at the monitoring point and the gradient curve of the hydrogen volume fraction at the outlet. Figure 9 shows the contours of hydrogen volume fraction at $Y = 12$ m and elbow.

From Table 7 and Figures 8 and 9, when the flow velocity increases from 5 to 9 m/s, the maximum hydrogen volume fraction decreased from 20.1757 to 20.1520%. At the horizontal pipe, because the density of methane is larger than that of hydrogen, under the influence of gravity, hydrogen gradually accumulates on the upper surface of the pipe along the direction of pipe length, and the hydrogen volume fraction is higher at the end of the pipe. The stratification phenomenon becomes less obvious with the increase of flow velocity. The hydrogen volume fraction gradient in gravity direction at the outlet decreases from 0.1722 to 0.1048. At the elbow, the stratification phenomenon is less obvious with the increase of flow velocity. This is due to the increase of the flow velocity, the more intense the gas movement, the more uniform the mixing of methane and hydrogen, the less prone it is to stratification. Therefore, in order to avoid stratification, hydrogenated natural gas is suitable for operation at high flow velocity.

3.2.3. Effect of Different Temperatures on the Flow of Hydrogen in the Elbow. Select group 3 to explore the influence of different temperatures on the flow of hydrogen in

https://doi.org/10.1021/acsomega.4c06890
ACS Omega 2024, 9, 47621−47636

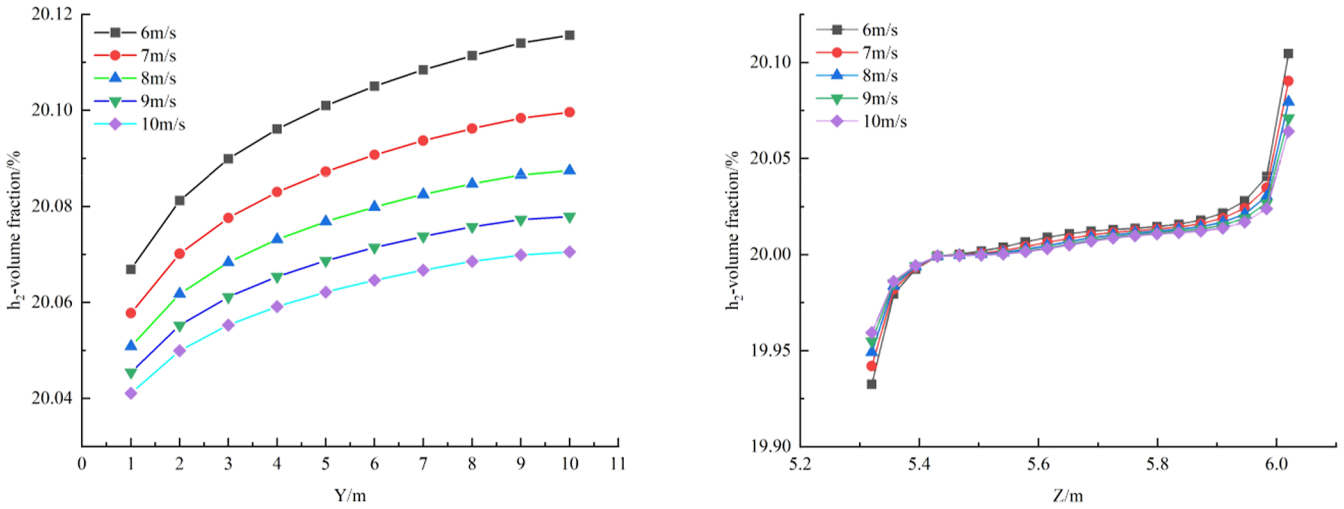

Figure 8. Variation curve of hydrogen volume fraction with *Y*-axis coordinates and the gradient diagram of hydrogen volume fraction under different flow velocities.

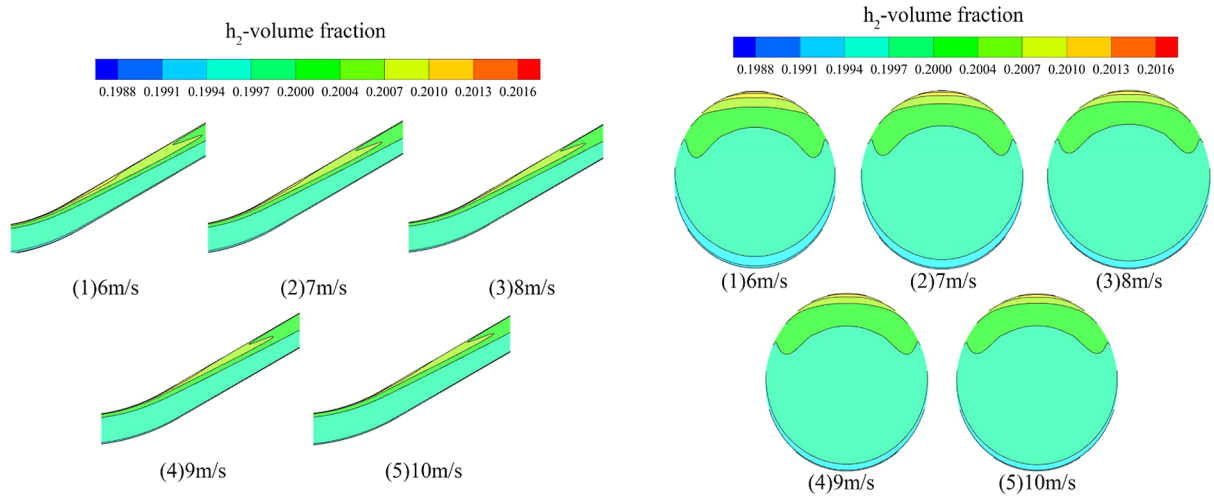

Figure 9. Distribution contours of hydrogen volume fraction at elbow under different flow velocities.

Table 8. Change of the Maximum Hydrogen Volume Fraction under Different Temperatures

influencing factor	temperature/(°C)	maximum hydrogen volume fraction/(%)	hydrogen volume in gravity direction/(10^{-2} m^{-1})
temperature	0	20.1765	0.1600
	10	20.1695	0.1540
	20	20.1628	0.1484
	30	20.1570	0.1431
	40	20.1510	0.1381

the elbow. Keeping other conditions unchanged, increase the temperature from 0 to 40 °C. The maximum hydrogen volume fraction under different temperatures and the gradient changes of the hydrogen volume fraction in gravity direction at the outlet are shown in Table 8. Figure 10 shows the variation curve of hydrogen volume fraction with *Y*-axis coordinates at the monitoring point and the gradient curve of the hydrogen volume fraction at the outlet. Figure 11 shows the contours of hydrogen volume fraction at $Y = 12$ m and elbow.

From Table 8 and Figures 10 and 11, when the temperature increases from 0 to 40 °C, the maximum hydrogen volume fraction decreased from 20.1765 to 20.1510%. At the horizontal pipe, because the density of methane is larger than that of hydrogen, under the influence of gravity, hydrogen gradually accumulates on the upper surface of the pipe along the direction of pipe length, and the hydrogen volume fraction is higher at the end of the pipe. The stratification phenomenon becomes less obvious with the increase of temperature. The hydrogen volume fraction gradient in the gravity direction at the outlet decreases from 0.1600 to 0.1381. At the elbow, the stratification phenomenon is less obvious with an increase of temperature. This is due to the increase of temperature leading to the decrease of gas density; gas molecules move more vigorously, and the more uniform the mixing of methane and hydrogen, the less prone to stratification.

3.2.4. Effect of Different Hydrogen Volume Fractions on the Flow of Hydrogen in the Elbow. Select group 4 to explore the influence of different hydrogen volume fractions on the

https://doi.org/10.1021/acsomega.4c06890
ACS Omega 2024, 9, 47621−47636

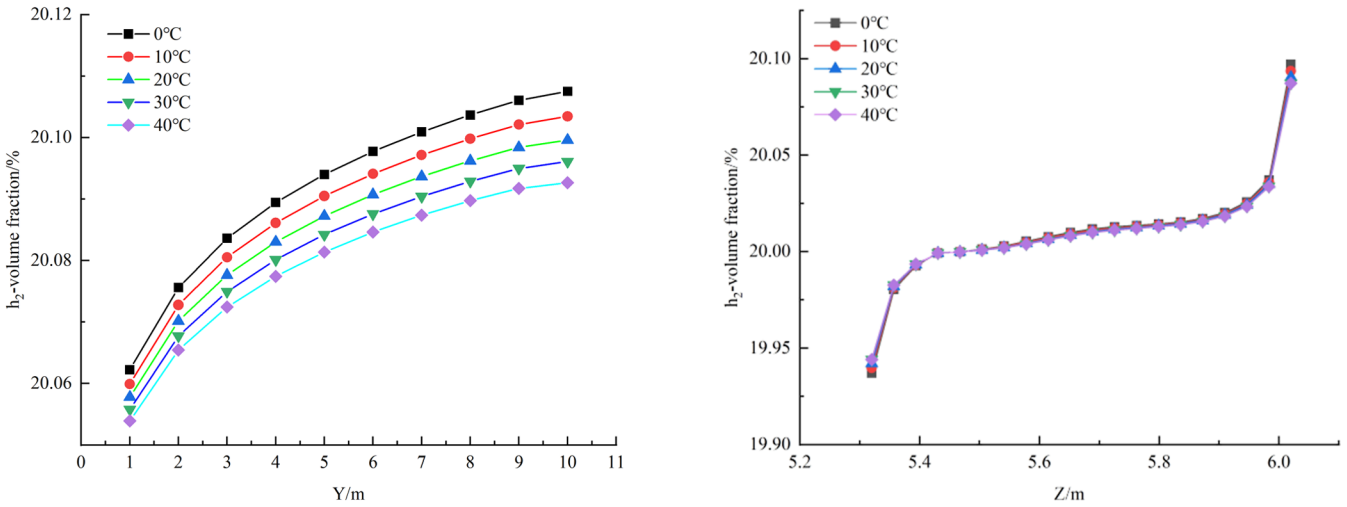

Figure 10. Variation curve of hydrogen volume fraction with *Y*-axis coordinates and the gradient diagram of hydrogen volume fraction under different temperatures.

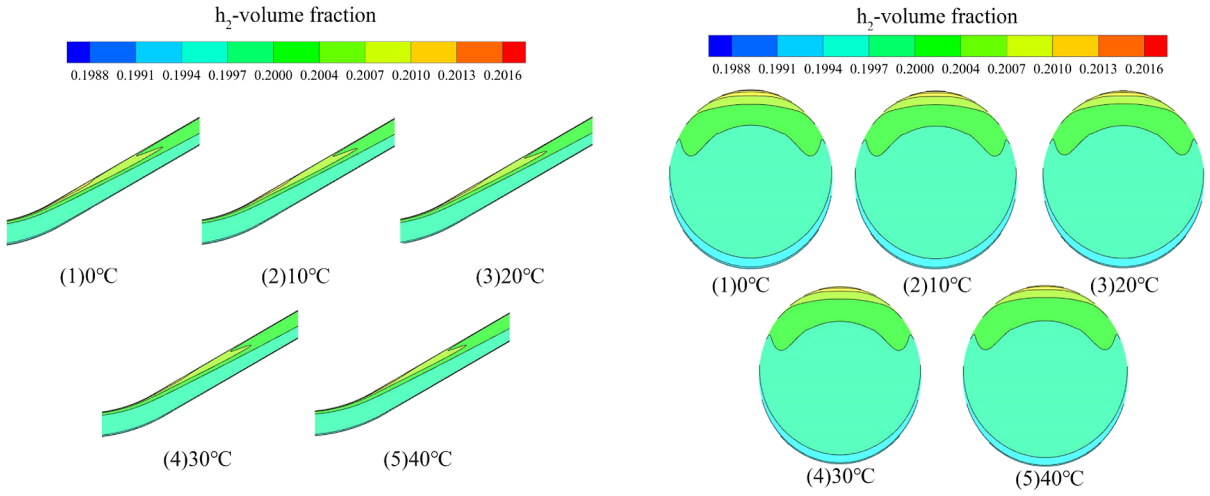

Figure 11. Distribution contours of hydrogen volume fraction at elbow under different temperatures.

Table 9. Change of the Maximum Hydrogen Volume Fraction under Different Hydrogen Volume Fractions

influencing factor	hydrogen volume fraction/(°C)	maximum hydrogen volume fraction/(%)	hydrogen volume in gravity direction/(10^{-2} m^{-1})
hydrogen volume fraction	10	10.1012	0.0932
	15	15.1363	0.1254
	20	20.1628	0.1484
	25	25.1807	0.1625
	30	30.1893	0.1692

flow of hydrogen in the elbow. Keeping other conditions unchanged, we increased the hydrogen volume fraction from 10 to 30%. The maximum hydrogen volume fraction under different pressures and the gradient changes of hydrogen volume fraction in gravity direction at the outlet are shown in Table 9. Figure 12 shows the variation curve of hydrogen volume fraction with *Y*-axis coordinates at the monitoring point and the gradient curve of the hydrogen volume fraction at the outlet. Figure 13 shows the contours of the hydrogen volume fraction at $Y = 12$ m and elbow.

From Table 9 and Figures 12 and 13, when the hydrogen volume fraction increased from 10 to 30%, the maximum hydrogen volume fraction decreased from 10.1012 to 30.1893%. At the horizontal pipe, hydrogen gradually accumulates on the upper surface of the pipe along the direction of pipe length, and the stratification phenomenon is more obvious with the increase of hydrogen volume fraction. The hydrogen volume fraction gradient in the gravity direction at the outlet increases from 0.0932 to 0.1692. At the elbow, the stratification phenomenon is more obvious with the increase of the hydrogen volume fraction. This is because with the increase of hydrogen volume fraction, the number of hydrogen molecules in the unit volume increases, resulting in the increase of hydrogen density and being more prone to stratification.

3.2.5. Effect of Different Undulating Angles on the Flow of Hydrogen in the Elbow. Select group 5 to explore the influence of different undulating angles on the flow of

https://doi.org/10.1021/acsomega.4c06890
ACS Omega 2024, 9, 47621−47636

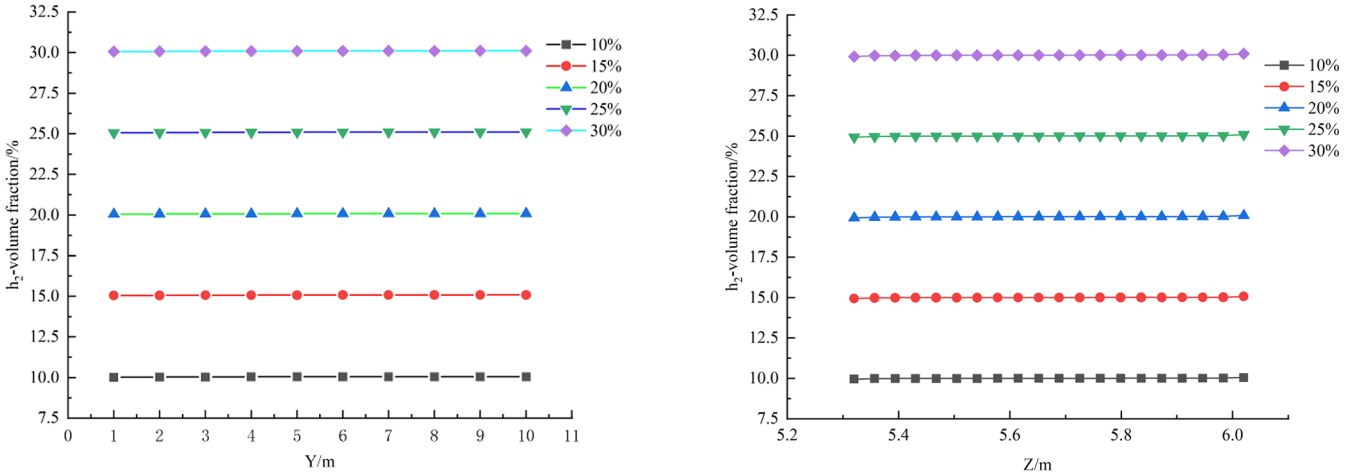

Figure 12. Variation curve of hydrogen volume fraction with *Y*-axis coordinates and the gradient diagram of hydrogen volume fraction under different hydrogen volume fractions.

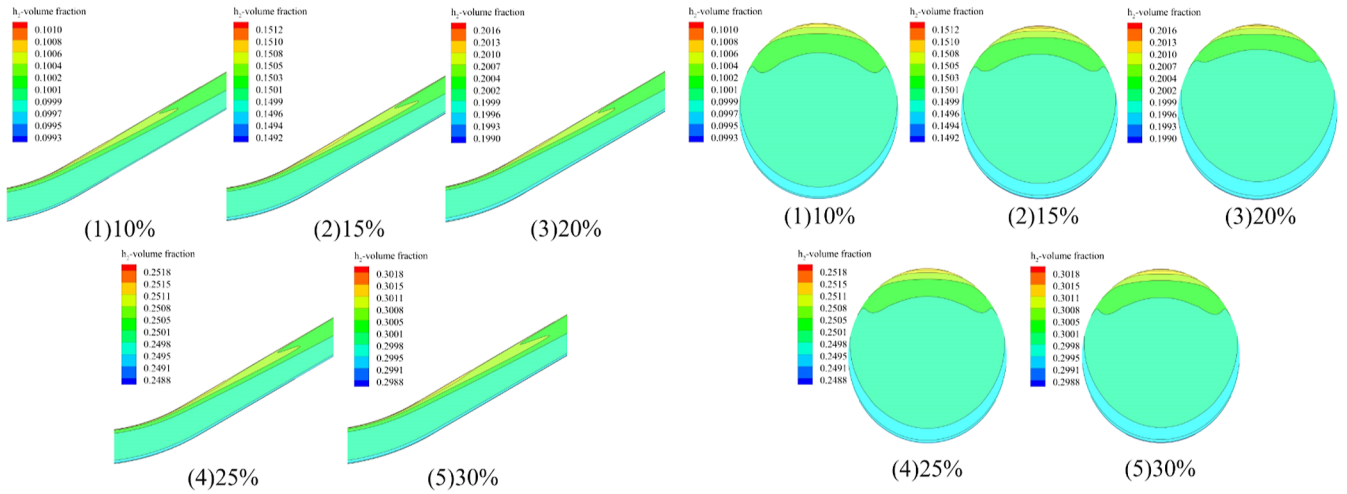

Figure 13. Distribution contours of hydrogen volume fraction at elbow under different hydrogen volume fractions.

Table 10. Change of the Maximum Hydrogen Volume Fraction under Different Undulating Angles

influencing factor	undulating angle/(deg)	maximum hydrogen volume fraction/(%)	hydrogen volume in gravity direction/(10^{-2} m^{-1})
undulating angle	30	20.1628	0.1484
	45	20.1834	0.0757
	60	20.1249	0.0453

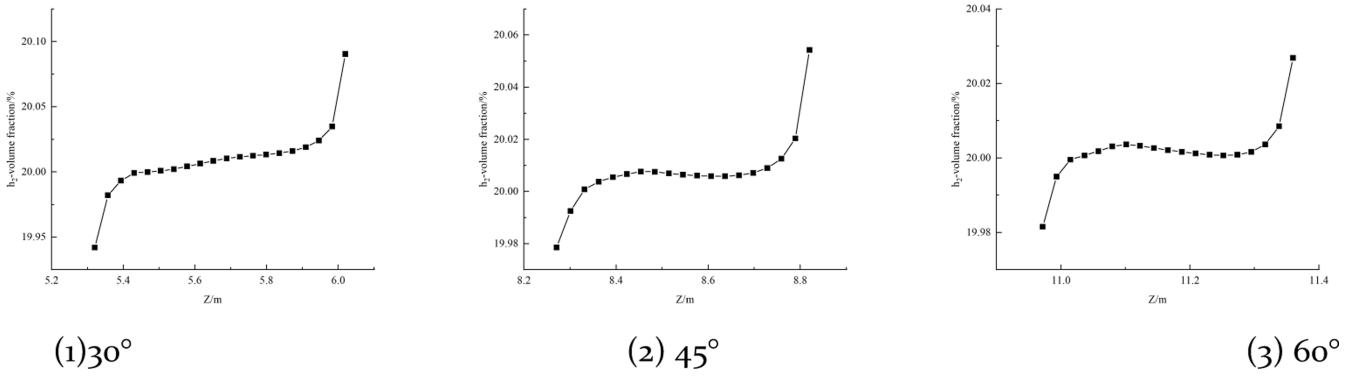

Figure 14. Hydrogen volume fraction gradient diagram at different undulating angles.

hydrogen in the elbow. Keeping other conditions unchanged, increase the undulating angle from 30° to 60°. The maximum hydrogen volume fraction under different undulating angles and the gradient changes of hydrogen volume fraction in

https://doi.org/10.1021/acsomega.4c06890
ACS Omega 2024, 9, 47621−47636

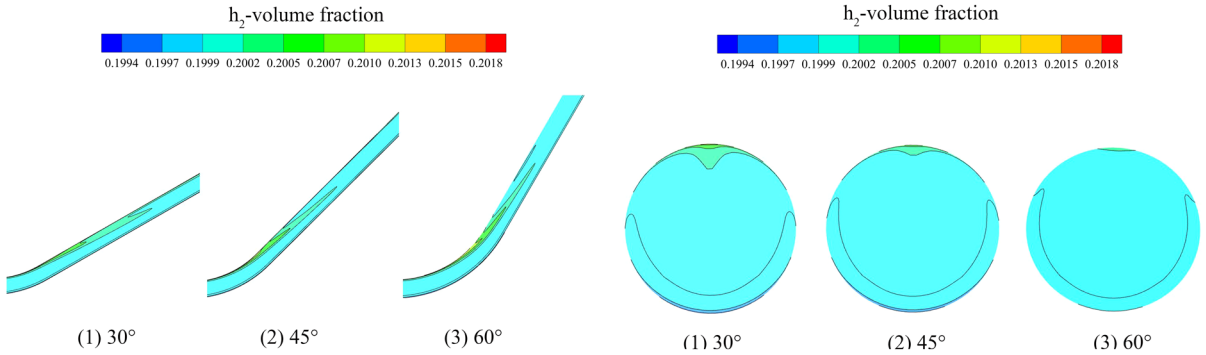

Figure 15. Distribution contours of hydrogen volume fraction at elbows and outlets with different undulating angles.

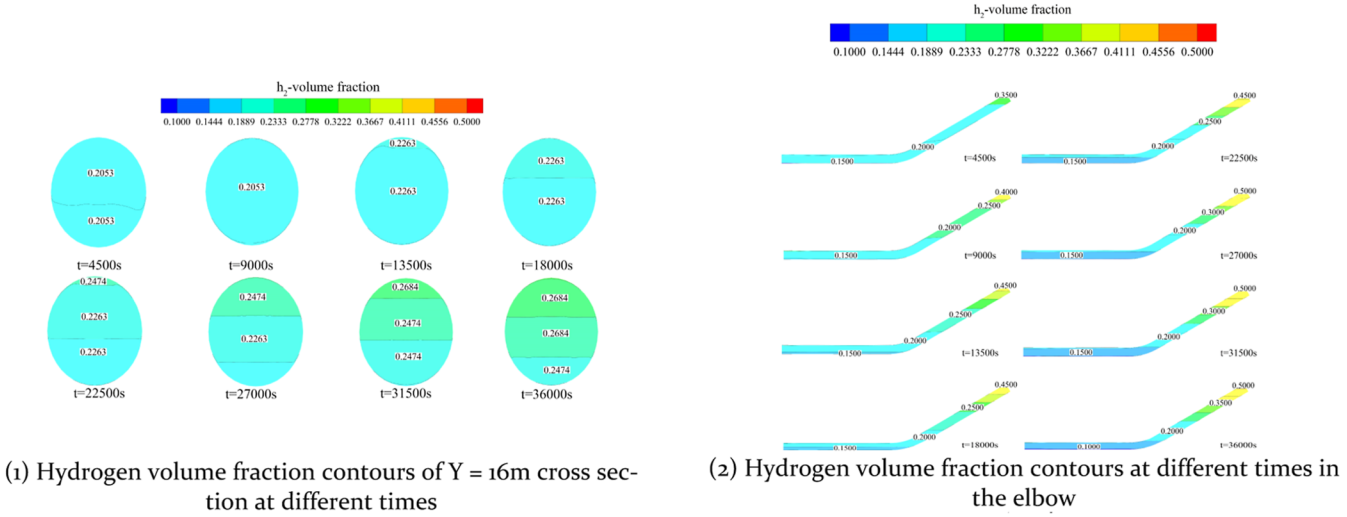

(1) Hydrogen volume fraction contours of Y = 16m cross section at different times

(2) Hydrogen volume fraction contours at different times in the elbow

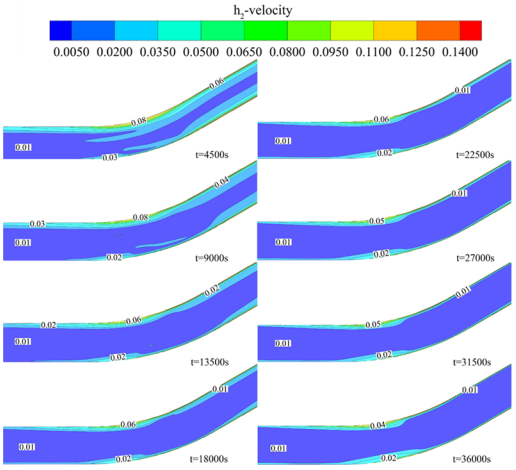

(3) Hydrogen slip rate contours at different times in the elbow

Figure 16. Hydrogen volume fraction contours and velocity contours in the elbow at different times.

gravity direction at the outlet are shown in Table 10. Figure 14 shows the hydrogen volume fraction gradient curve at the outlet. Figure 15 shows the distribution contours of the hydrogen volume fraction at elbows and outlets with different undulating angles.

From Table 10 and Figures 14 and 15, at the outlet, because the density of methane is larger than that of hydrogen, hydrogen gradually accumulates on the upper surface of the pipe along the length direction of the pipe, and the volume fraction of hydrogen at the end of the pipe is higher. When the undulating angle increases from 30° to 60°, at the elbow, the stratification phenomenon is less obvious with the increase of the undulating angle. The gradient of hydrogen volume fraction in gravity direction at the outlet decreases from 0.1484 to 0.0453. This is because with the increase of the undulating angle, the stronger the turbulent effect of hydrogen

https://doi.org/10.1021/acsomega.4c06890
ACS Omega 2024, 9, 47621−47636

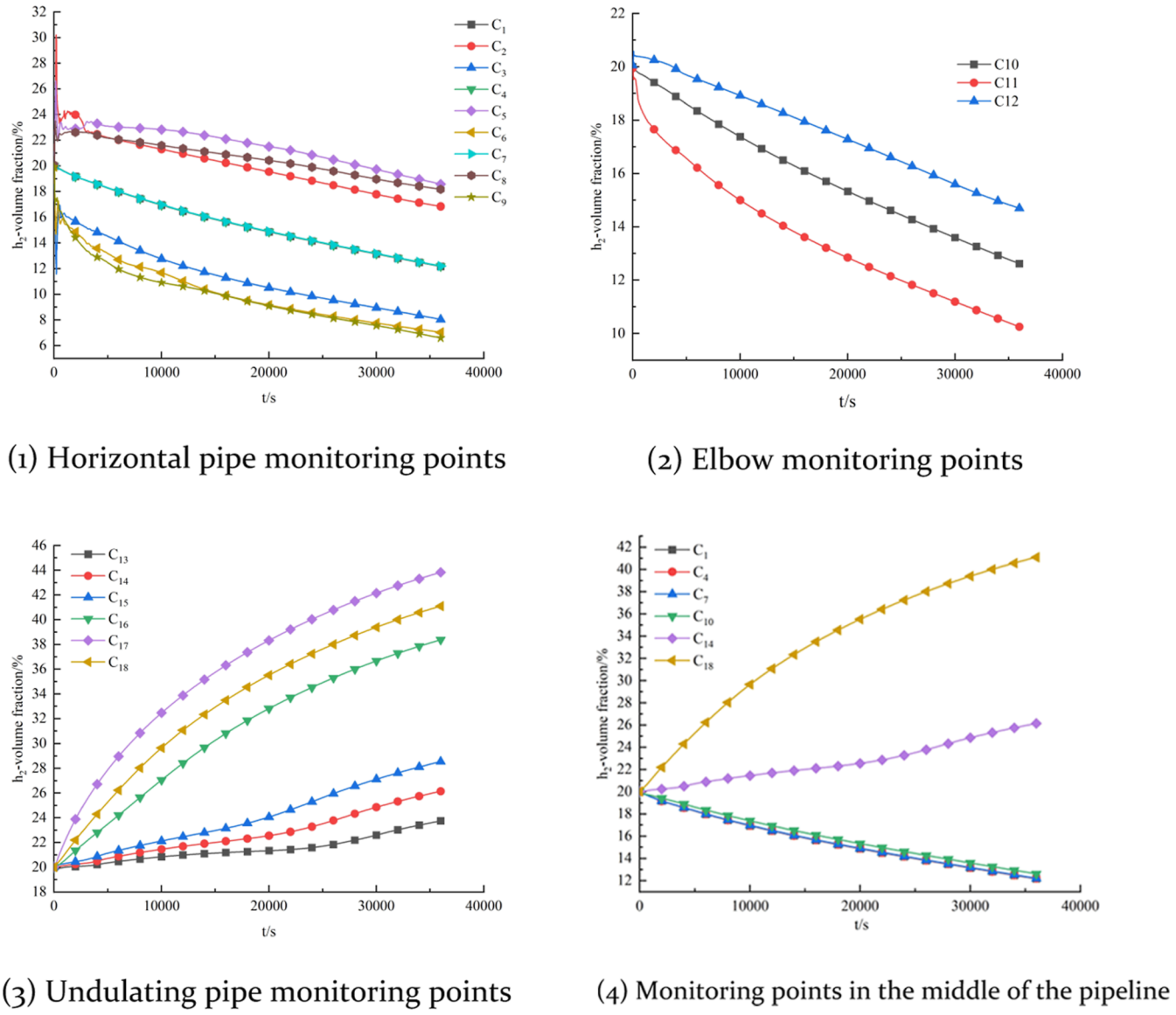

Figure 17. Change of hydrogen volume fraction with time at different monitoring points.

Table 11. Horizontal Pipe Monitoring Point Coordinates

Monitoring point/(m)	C_1	C_2	C_3	C_4	C_5	C_6	C_7	C_8	C_9
X	0	0	0	0	0	0	0	0	0
Y	3	3	3	6	6	6	9	9	9
Z	0	0.405	−0.405	0	0.405	−0.405	0	0.405	−0.405

at the elbow, the more uniform the mixing, and the less prone to stratification.

4. STUDY ON THE DISTRIBUTION OF HYDROGEN CONCENTRATION UNDER THE CONDITION OF SHUTDOWN OF ELBOWS

4.1. Analysis of Elbow Shutdown Characteristics. In order to explore the research on the distribution of hydrogen concentration in the elbow from the running state to the shutdown state, based on the working conditions of Table 3, the outlet and inlet are set as the wall for the unsteady calculation, and the time step is 0.02. The contours of the hydrogen volume fraction distribution and velocity distribution at different times are shown in Figure 16.

From Figure 16, it can be seen that the volume fraction of hydrogen in horizontal pipes and elbows gradually decreases within 0 s < $t \leq$ 36000 s. Hydrogen gradually accumulates in the upper part of the undulating pipeline, and the maximum volume fraction of hydrogen reaches about 55.66%. The hydrogen volume fraction is distributed in a horizontal concentration gradient along the vertical direction and gradually accumulates at the height of the undulating pipe, and the stratification phenomenon is obvious. With the passage of time, the slip rate of hydrogen gradually decreases. The flow velocity at the elbow and the undulating pipe is faster than that at the horizontal pipe, and the closer to the pipe wall, the faster the flow velocity. At the wall, the hydrogen slip rate is about

https://doi.org/10.1021/acsomega.4c06890
ACS Omega 2024, 9, 47621−47636

Table 12. Elbow, Undulating Pipe Monitoring Point Coordinates

monitoring point/(m)	C_{10}	C_{11}	C_{12}	C_{13}	C_{14}	C_{15}	C_{16}	C_{17}	C_{18}
X	0	0	0	0	0	0	0	0	0
Y	11	11	11	16	16	16	20	20	20
Z	0.1	−0.3	0.5	2.3	2.7	3.1	4.6	5.4	5.0

Table 13. Maximum/Low Hydrogen Volume Fraction and Concentration Difference at Different Hydrogen Volume Fractions

influencing factor	hydrogen volume fraction/(%)	maximum hydrogen volume fraction/(%)	minimum hydrogen volume fraction/(%)	concentration difference/(%)
hydrogen volume fraction	10	43.4366	1.2835	42.1531
	15	50.4006	2.9266	47.4740
	20	55.6613	5.1890	50.4723
	25	59.9226	8.0551	51.8675
	30	63.4974	11.6346	51.8628

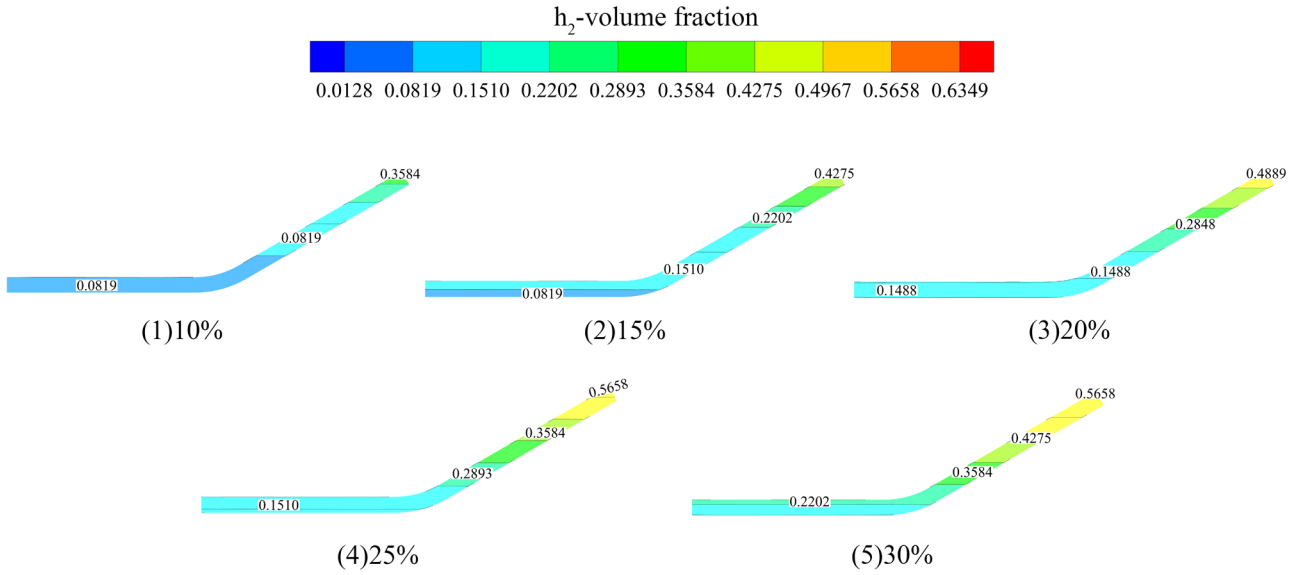

Figure 18. Axial cross-section contours of the elbow at t = 36000 s under different hydrogen volume fractions.

0.04 m/s, and the flow velocity in the center of the pipe is about 0.01 m/s.

The monitoring points C_1, C_2, C_3, C_4, C_5, C_6, C_7, C_8, and C_9 are set in the horizontal pipe. The monitoring points C_{10} and C_{11} are set in the elbow. The monitoring points C_{12}, C_{13}, C_{14}, C_{15}, C_{16}, C_{17}, and C_{18} are set in the undulating pipe. The specific coordinates are shown in Tables 11 and 12. The curves of hydrogen volume fraction at monitoring points at horizontal pipe, elbow pipe, and undulating pipe with time and hydrogen volume fraction at monitoring points in the middle of the pipeline with time are shown in Figure 17.

From Figure 17(1), 4−2(2) and 4−2(3), in the horizontal pipe, when t < 2000 s, the variation of hydrogen volume fraction fluctuated significantly. When $t \geq 2000$ s, the decline trend of hydrogen volume fraction gradually stabilized. Hydrogen accumulates on the upper surface of the pipeline, and the difference of hydrogen volume fractions between the upper surface and the lower surface was about 11.00%. In the elbow, the decreasing trend of hydrogen volume fraction is gradually gentle, and the difference of hydrogen volume fractions between the upper surface and the lower surface was about 5.00%. In the undulating pipe, the rising trend of hydrogen volume fraction is gradually gentle, and the hydrogen volume fraction increases with the increase of height. The difference of hydrogen volume fraction between the upper surface and the lower surface was about 5.00%.

From Figure 17(4), due to the different densities of methane and hydrogen, the hydrogen gradually moves higher. The hydrogen volume fraction in the horizontal pipe and elbow gradually decreases, and the change trend is basically the same. The hydrogen volume fraction in the undulating pipe gradually increases, and the higher the height, the faster the increase. With the extension of shutdown time, the growth of the hydrogen volume fraction gradually slows down.

4.2. Influence of Different Hydrogen Volume Fractions on Hydrogen under the Condition of Elbow Shutdown. The increase of hydrogen volume fraction will aggravate the hydrogen damage of the pipeline and lead to pipe failure. Based on this, the influence of five different hydrogen volume fractions on hydrogen in the state of elbow shutdown was studied. The volume fraction of hydrogen is 10, 15, 20, 25, and 30%, respectively. The maximum hydrogen volume fraction, the minimum hydrogen volume fraction, and the concentration difference under different hydrogen volume fractions are shown in Table 13. Figure 18 shows the axial cross-section contours of the elbow at t = 36000 s under different hydrogen volume fractions. Figure 19 shows the variation curve of the hydrogen volume fraction in the middle of the elbow under different hydrogen volume fractions. Figure

https://doi.org/10.1021/acsomega.4c06890
ACS Omega 2024, 9, 47621−47636

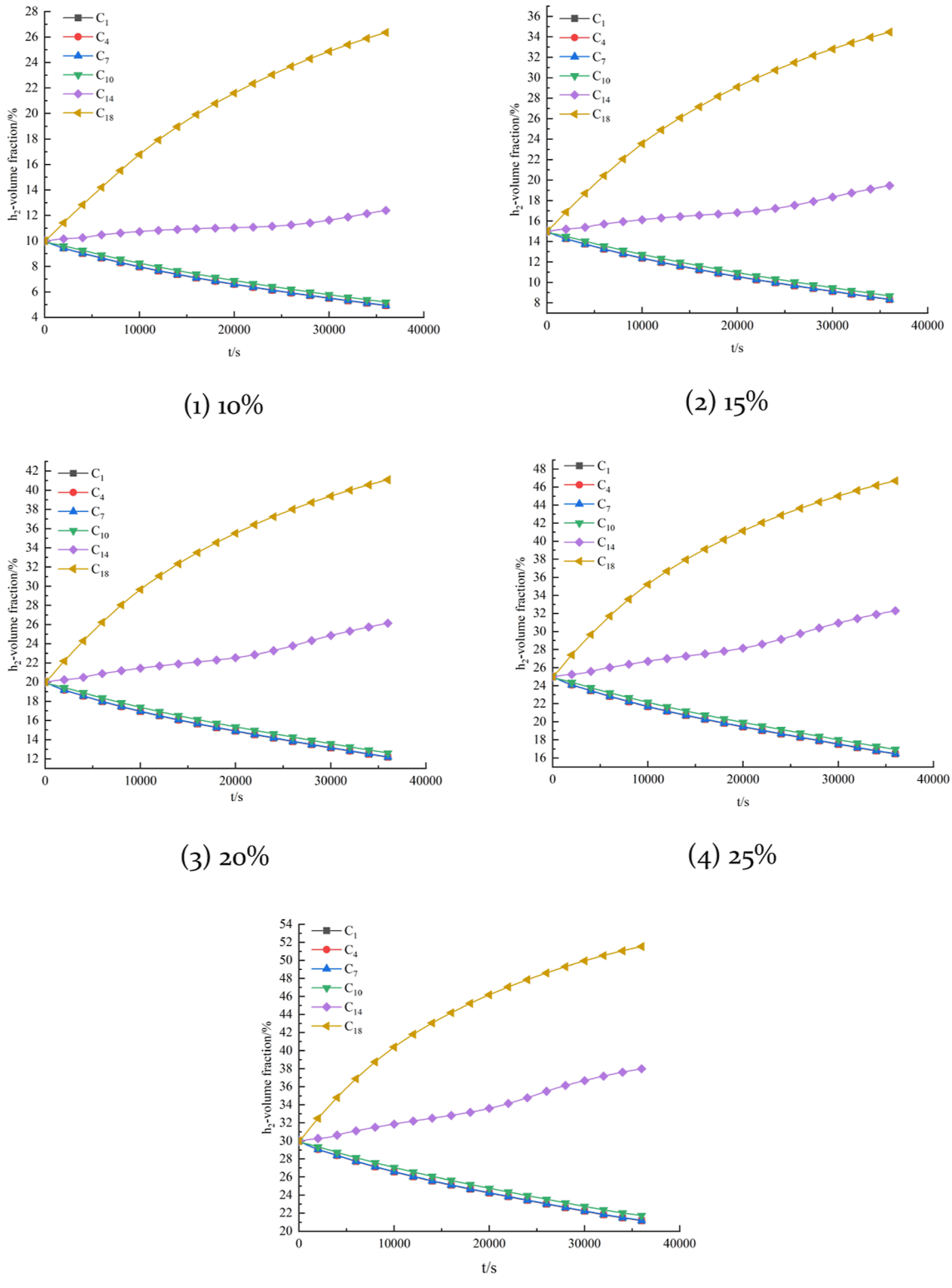

Figure 19. Variation curve of hydrogen volume fraction in the middle of the elbow under different hydrogen volume fractions.

20 shows the hydrogen volume fraction change with time and the concentration difference at monitoring point 18.

From Table 13 and Figures 18, 19, and 20, because the density of methane is higher than that of hydrogen, hydrogen gradually accumulates on the upper surface of the pipe along the pipe length direction, and the volume fraction of hydrogen at the end of the pipe is higher. With the increase of hydrogen volume fraction, the maximum hydrogen volume fraction gradually increases, and the concentration difference increases gradually and finally becomes stable. When the hydrogen volume fraction increases from 10 to 30%, the concentration gradient of the hydrogen volume fraction in the gravity

https://doi.org/10.1021/acsomega.4c06890
ACS Omega 2024, 9, 47621−47636

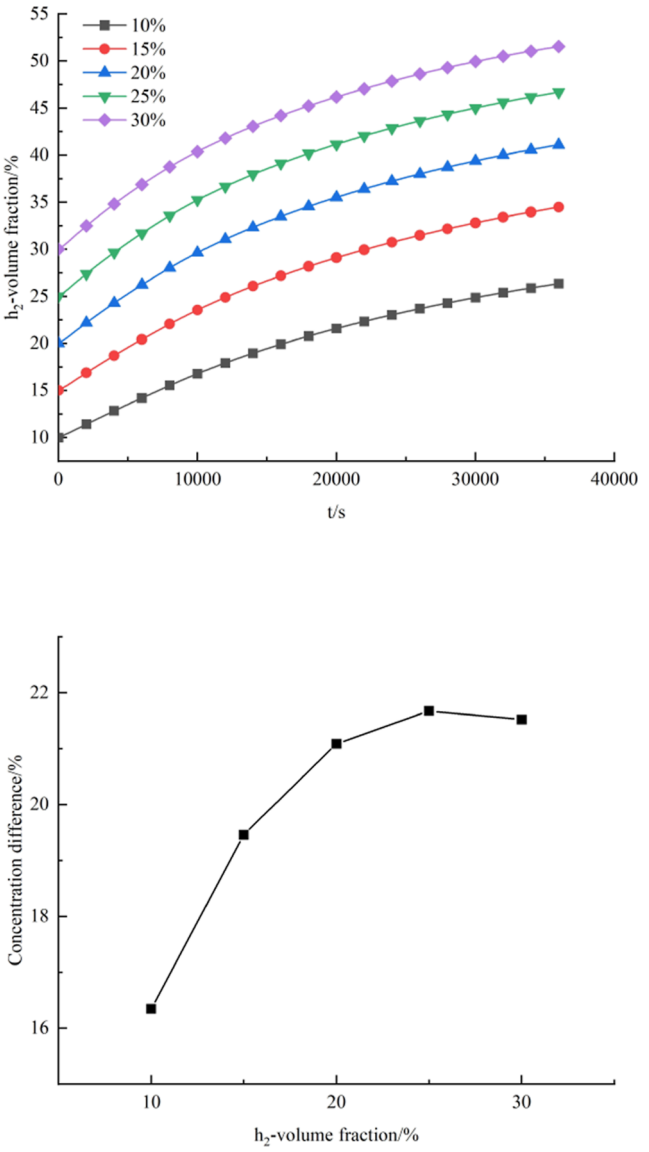

Figure 20. Hydrogen volume fraction change with time and the concentration difference at monitoring point 18.

direction increases from 0.2765 to 0.3436. The decrease of hydrogen volume fraction in the horizontal pipe increases from 5.05 to 8.78%. The decrease of hydrogen volume fraction in the elbow increases from 4.80 to 8.26%. The increase of hydrogen volume fraction in the undulating pipe increases from 16.34 to 21.52%. The stratification phenomenon is gradually obvious with the increase of hydrogen volume fractions.

5. RESULTS AND DISCUSSION

This paper focuses on the flow characteristics of HCNG in an elbow under operation and shutdown conditions. The main conclusions are summarized as follows:

(1) During the flow of HCNG in the elbow, due to the different physical and chemical properties of methane and hydrogen, the lighter density hydrogen gradually moves above the pipe, and the heavier density methane gradually moves below the pipe. The stratification of hydrogen in gravity direction along the length direction of the pipe is gradually obvious, and the closer to the center of the pipe, the more uniform the hydrogen distribution. The velocity of hydrogen at the elbow and the undulating pipe is faster than that of the horizontal pipe, and the closer to the wall, the lower the velocity. The stratification phenomenon increases with the increase of pressure and hydrogen volume fraction and the decrease of flow velocity, temperature, and undulating angle. The hydrogen volume fraction varies within 0.2% with pressure, flow velocity, temperature, hydrogen volume fraction, and undulating angle, and the nonuniform distribution of hydrogen in the elbow can be ignored.

(2) When the HCNG is shutdown in the elbow, with the extension of shutdown time, the volume fraction of hydrogen at the horizontal pipe and elbow decreases. Hydrogen gradually accumulates in the upper part of the undulating pipe and distributes in a horizontal concentration gradient along the vertical direction, with obvious stratification. With the extension of shutdown time, the growth of the hydrogen volume fraction gradually slowed down. With the passage of time, the slip rate of hydrogen and methane appears under the influence of the density difference and gradually weakens. The closer to the pipe wall, the greater the slip rate. With the increase of hydrogen volume fraction, the maximum hydrogen volume fraction increases gradually, and the stratification phenomenon is gradually obvious.

(3) In the process of hydrogen blending transportation, attention should be paid to the hydrogen accumulation area in the elbow to avoid safety accidents. The static mixer or disturbance elements are added to improve the mixing uniformity of methane and hydrogen. The calculation results in this paper can provide theoretical support for the maintenance of HCNG elbows from operation to shutdown.

■ ASSOCIATED CONTENT

Data Availability Statement

All data are provided within the manuscript. To request data for this study, please contact the corresponding author.

■ AUTHOR INFORMATION

Corresponding Author

Gang Liu − *College of Safety Science and Engineering, Chongqing University of Science & Technology, Chongqing 401331, China;* orcid.org/0000-0002-6476-3395; Email: liugang@cqust.edu.cn

Authors

Jiuqing Ban − *Natural Gas Research Institute, PetroChina Southwest Oil & Gas Field Company, Chengdu 610213, China; Key Laboratory of Natural Gas Quality Control and Energy Measurement for State Market Regulation, Chengdu 610213, China;* orcid.org/0000-0003-4586-8121

Li Zhou − *Natural Gas Research Institute, PetroChina Southwest Oil & Gas Field Company, Chengdu 610213, China; Key Laboratory of Natural Gas Quality Control and Energy Measurement for State Market Regulation, Chengdu 610213, China*

Yun Jiang − *PetroChina Southwest Oil & Gas Field Company, Chengdu 610000, China*

https://doi.org/10.1021/acsomega.4c06890
ACS Omega 2024, 9, 47621−47636

Yan Wu − *PipeChina West-East Gas Pipeline Company, Shanghai 200122, China*
Wei Yang − *Natural Gas Research Institute, PetroChina Southwest Oil & Gas Field Company, Chengdu 610213, China; Key Laboratory of Natural Gas Quality Control and Energy Measurement for State Market Regulation, Chengdu 610213, China*
Duo Chen − *College of Safety Science and Engineering, Chongqing University of Science & Technology, Chongqing 401331, China*

Complete contact information is available at: https://pubs.acs.org/10.1021/acsomega.4c06890

Author Contributions

J.Q.B.: writing—original draft and writing—review and editing. G.L.: methodology and writing—review and editing. L.Z., Y.J., Y.W., and W.Y.: project administration and supervision and formal analysis. D.C.: formal analysis.

Notes

The authors declare no competing financial interest.

■ ACKNOWLEDGMENTS

This research was funded by the Postdoctoral Foundation of PetroChina Southwest Oil and Gas Field Company (grant no. 20230312-10).

■ REFERENCES

(1) Baykara, S. Z. Hydrogen: a brief overview on its sources, production and environmental impact. *Int. J. Hydrogen Energy* **2018**, *43* (23), 10605−10614.
(2) Le, P. A.; Trung, V. D.; Nguyen, P. L.; Bac Phung, T. V.; Natsuki, J.; Natsuki, T. The current status of hydrogen energy: an overview. *RSC Adv.* **2023**, *13* (40), 28262−28287.
(3) Okolie, J. A.; Patra, B. R.; Mukherjee, A.; Nanda, S.; Dalai, A. K.; Kozinski, J. A. Futuristic applications of hydrogen in energy, biorefining, aerospace, pharmaceuticals and metallurgy. *Int. J. Hydrogen Energy* **2021**, *46*, 8885−8905.
(4) Omid, M. A.; Sahin, M. E.; Cora, Ö. N. Challenges and Future Perspectives on Production, Storage Technologies, and Transportation of Hydrogen: A Review. *Energy Technol.* **2024**, *12* (4), 2300997.
(5) Xu, X. X.; Zhou, Q.; Yu, D. H. The future of hydrogen energy: Bio-hydrogen production technology. *Int. J. Hydrogen Energy* **2022**, *47* (79), 33677−33698.
(6) Zhang, C. Y.; Shao, Y. B.; Shen, W. P.; Li, H.; Nan, Z.; Dong, M.; Bian, J.; Cao, X. Key Technologies of Pure Hydrogen and Hydrogen-Mixed Natural Gas Pipeline Transportation. *ACS Omega* **2023**, *8* (22), 19212−19222.
(7) Peng, S. B.; Luo, X.; Yang, L. Numerical simulation of leakage and diffusion law of hydrogen-doped natural gas long-distance pipeline. *Chem. Eng. Oil Gas* **2023**, *52* (06), 44−52 + 59.
(8) Sharma, S.; Basu, S.; Shetti, N. P.; Aminabhavi, T. M. Waste-to-energy nexus for circular economy and environmental protection: Recent trends in hydrogen energy. *Sci. Total Environ.* **2020**, *713*, 136633.
(9) Ishaq, H.; Dincer, I.; Crawford, C. A review on hydrogen production and utilization: Challenges and opportunities. *Int. J. Hydrogen Energy* **2022**, *47* (62), 26238−26264.
(10) Zhang, P. Y.; Luo, Q.; Zhou, L.; Wang, H. L. Discussion on the adaptability of hydrogen blending in domestic natural gas analysis and testing standards. *Chem. Eng. Oil Gas* **2023**, *52* (03), 103−106 + 117.
(11) Chen, Y. Y.; Long, L. W.; Niu, J.; Huang, T. M.; Chen, X.; Zhang, J.; Wan, Z.; Yu, B. Investigation on the Combustion Characteristics and Environmental Effects of Hydrogen-doped Natural Gas for Domestic Water Heaters. *ACS Omega* **2023**, *8* (50), 48370−48380.
(12) Wang, X.; Chen, S. P.; Zhu, N. Development status and prospect of liquid hydrogen storage and transportation technology. *Acta Energ. Sol. Sin.* **2024**, *45* (01), 500−514.
(13) Rao, Y. C.; Hu, Y.; Wang, S. L.; Li, F.; Su, W. J. The development status and existing problems of liquid hydrogen storage and transportation technology. *Mod. Chem. Ind.* **2023**, *43* (06), 6−11.
(14) Aziz, M. Liquid Hydrogen: A Review on Liquefaction, Storage, Transportation, and Safety. *Energies* **2021**, *14* (18), 5917.
(15) Li, Y. X.; Zhou, H.; Zhu, J. L.; Liu, C. W.; Lv, H.; Peng, W.; Lu, S.; Li, L. L. Decompression and pressure regulation of pure hydrogen/hydrogen-doped natural gas pipeline. *Oil Gas Storage Transp.* **2024**, *43* (01), 21−31.
(16) Zhang, C. Y.; Shao, Y. B.; Shen, W. P.; Li, H.; Nan, Z. L.; Dong, M. Q.; Bian, J.; Cao, X. W. Key Technologies of Pure Hydrogen and Hydrogen-Mixed Natural Gas Pipeline Transportation. *ACS Omega* **2023**, *8* (22), 19212−19222.
(17) Di Lullo, G.; Giwa, T.; Okunlola, A.; Davis, M.; Mehedi, T.; Oni, A.; Kumar, A. Large-scale long-distance land-based hydrogen transportation systems: A comparative techno-economic and greenhouse gas emission assessment. *Int. J. Hydrogen Energy* **2022**, *47* (83), 35293−35319.
(18) Kong, Y. Y.; Cui, J. T.; Han, H.; Liu, C. W.; Duan, P. F.; Han, J. K.; Li, Y. X. Comparative analysis and discussion on domestic and foreign technical standards for hydrogen pipeline transportation. *Oil Gas Storage Transp.* **2023**, *42* (08), 944−951.
(19) Li, F.; Dong, S. H.; Chen, L.; Zhu, X. P.; Han, Z. C. Key safety technologies and progress in long-distance pipeline transportation of hydrogen-blended natural gas. *Mech. Eng.* **2023**, *45* (02), 230−244.
(20) Zhong, B.; Zhang, X. X.; Zhang, B.; Peng, S. P. Industrial Development of Hydrogen Blending in Natural Gas Pipelines in China. *Strategic Study of CAE* **2022**, *24* (3), 100−107.
(21) Chae, M. J.; Kim, J. H.; Moon, B.; Park, S.; Lee, Y. S. The present condition and outlook for hydrogen-natural gas blending technology. *Korean J. Chem. Eng.* **2022**, *39*, 251−262.
(22) Song, P. F.; Shan, T. W.; Li, Y. W.; Hou, J. G.; Wang, X. L.; Zhang, D. The influence of hydrogen blending in natural gas pipeline and its technical feasibility analysis. *Mod. Chem. Ind.* **2020**, *40* (07), 5−10.
(23) Tian, X.; Pei, J. J. Study progress on the pipeline transportation safety of hydrogen-blended natural gas. *Heliyon* **2023**, *9* (11), 21454.
(24) Messaoudani, L. Z.; Rigas, F.; Hamid, B. D. M.; Hassan, C. R. C. Hazards, safety and knowledge gaps on hydrogen transmission via natural gas grid: A critical review. *Int. J. Hydrogen Energy* **2016**, *41* (39), 17511−17525.
(25) Giovanni, L. D.; Olufemi, A. O.; Amit, K. Blending blue hydrogen with natural gas for direct consumption: Examining the effect of hydrogen concentration on transportation and well-to-combustion greenhouse gas emissions. *Int. J. Hydrogen Energy* **2021**, *46* (36), 9202−19216.
(26) Zhang, H. Y.; Diao, R.; Luo, X. M.; Xie, Q. Molecular simulation of H2/CH4 mixture storage and adsorption in kaolinite nanopores for underground hydrogen storage. *ACS Omega* **2023**, *8* (48), 45801−45816.
(27) Zheng, L.; Fu, J. Y. Development status of high grade pipeline steel. *Iron Steel* **2006**, *10*, 1−10.
(28) Liu, C. W.; Pei, Y. B.; Cui, Z. X.; Li, X. J.; Yang, H. C.; Xing, X.; Duan, P. F.; Li, L. I.; Li, Y. X. Study on the stratification of the blended gas in the pipeline with hydrogen into natural gas. *Int. J. Hydrogen Energy* **2023**, *48* (13), 5186−5196.
(29) Zhao, B. X.; Peng, X. Adaptability analysis of steel pipe and material of hydrogen long-distance pipeline. *Mod. Chem. Ind.* **2017**, *37* (05), 217−219.
(30) Wu, X.; Zhang, H. F.; Yang, M.; Jia, W. L.; Qiu, Y. Z.; Lan, L. From the perspective of new technology of blending hydrogen into natural gas pipelines transmission: mechanism, experimental study, and suggestions for further work of hydrogen embrittlement in high-strength pipeline steels. *Int. J. Hydrogen Energy* **2022**, *47* (12), 8071−8090.

(31) An, Y. W.; Sun, C.; Ji, S. H.; Jia, G. W.; Xu, W. Q.; Liu, W.; Zhou, L.; Cai, M. L. Hydrogen concentration distribution of natural gas mixed with hydrogen in pipeline flow. *Mech. Eng.* **2022**, *44* (04), 767−775.
(32) Wang, S.; Yang, C. G.; Zhou, H.; Niu, B. Y.; Li, J. N.; Luo, T. T. Numerical simulation study on flow characteristics of hydrogen blending transportation in T-type natural gas pipeline. *J. Yanbian Univ., Nat. Sci. Ed.* **2023**, *42* (04), 1−8.
(33) Li, J.; Sun, C. Y.; Liang, G.; Fei, T.; Zhang, C. L.; Yang, W. Y.; Song, K. Study on the influence of deformation of undulating section of hydrogen pipeline on flow field. *Electrical Age* **2023**, *S1*, 55−58.
(34) Liu, C. W.; Cui, Z. X.; Zhang, J. X.; Pei, Y. B.; Duan, P. F.; Li, L. L.; Yang, H. C.; Li, Y. X. The stratification phenomenon of hydrogen-blended natural gas pipeline. *J. China Univ. Pet., Ed. Nat. Sci.* **2022**, *46* (05), 153−161.
(35) Ji, S. H.; Sun, C.; An, Y. W.; Yan, S. J.; Jia, G. W.; Xu, W. Q.; Liu, W.; Li, M. X.; Cai, M. L. Study on the adaptability of ultrasonic flowmeter to the structure of hydrogen-doped natural gas pipeline. *Mech. Eng.* **2023**, *45* (02), 333−344.
(36) Marangon, A.; Carcassi, M. Hydrogen−methane mixtures: Dispersion and stratification studies. *Int. J. Hydrogen Energy* **2014**, *39* (11), 6160−6168.
(37) Ren, S. Y. Study on the law of natural gas mixing and explosion propagation in confined space. *J. Saf. Sci. Technol.* **2016**, *12* (11), 130.
(38) Ren, S. Y. *Study on gas mixing and flammability in confined space*; Beijing Institute Of Technology: Beijing, 2016.
(39) Chen, J. W.; Shang, J.; Liu, Y. J.; Liu, L. S.; Tang, X. Y.; Zhu, H. J.; Guo, Y. L.; Peng, F. Y. Discussion on Safety Design Points of Mixed Hydrogen Natural Gas Pipeline. *Nat. Gas Oil* **2020**, *38* (06), 8−13.
(40) Zhu, H. J.; Chen, J. W.; Su, H. Z.; Tang, T.; He, S. Numerical study on static stratification process of gas in undulating natural gas hydrogen-doped pipeline. *J. Southwest Pet. Univ.* **2022**, *44* (06), 132−140.
(41) Zhang, X. Q.; Jiang, Q. M. Adaptability analysis of adding hydrogen pipe to existing natural gas pipeline. *Pressure Vessel Technol.* **2015**, *32* (10), 17−22.
(42) Dai, W. S. The selection of flow rate of hydrogen pipeline in oil refining enterprises and the requirements of GB 50177−2005 'Design Code for Hydrogen Station' on the flow rate of hydrogen pipeline. *Stand. Sci.* **2020**, *01*, 65−69 + 86.

https://doi.org/10.1021/acsomega.4c06890
ACS Omega 2024, 9, 47621−47636